Eur. J. Biochem. **270**, 3018–3025 (2003) © FEBS 2003 doi:10.1046/j.1432-1033.2003.03679.x

Identification of a novel binding site for calmodulin in ammodytoxin A, a neurotoxic group IIA phospholipase A_2

Petra Prijatelj[1], Jernej Šribar[2], Gabriela Ivanovski[2], Igor Križaj[2], Franc Gubenšek[1,2] and Jože Pungerčar[2]

[1]*Department of Chemistry and Biochemistry, Faculty of Chemistry and Chemical Technology, University of Ljubljana, Ljubljana, Slovenia;* [2]*Department of Biochemistry and Molecular Biology, Jožef Stefan Institute, Ljubljana, Slovenia*

The molecular mechanism of the presynaptic neurotoxicity of snake venom phospholipases A_2 (PLA_2s) is not yet fully elucidated. Recently, new high-affinity binding proteins for PLA_2 toxins have been discovered, including the important intracellular Ca^{2+} sensor, calmodulin (CaM). In the present study, the mode of interaction of group IIA PLA_2s with the Ca^{2+}-bound form of CaM was investigated by mutational analysis of ammodytoxin A (AtxA) from the long-nosed viper (*Vipera ammodytes ammodytes*). Several residues in the C-terminal part of AtxA were found to be important in this interaction, particularly those in the region 115–119. In support of this finding, introduction of Y115, I116, R118 and N119, present in AtxA, into a weakly neurotoxic PLA_2 from Russell's viper (*Daboia russellii russellii*) increased by sevenfold its binding affinity for CaM. Furthermore, two out of four peptides deduced from different regions of AtxA were able to compete with the toxin in binding to CaM. The nonapeptide showing the strongest inhibition was that comprising the AtxA region 115–119. This stretch contributes to a distinct hydrophobic patch within the region 107–125 in the C-terminal part of the molecule. This lacks any substantial helical structure and is surrounded by several basic residues, which may form a novel binding motif for CaM on the molecular surface of the PLA_2 toxin.

Keywords: *Daboia russellii russellii*; neuronal receptor; snake venom; toxicity; *Vipera ammodytes ammodytes*.

Introduction

Phospholipases A_2 (PLA_2s, EC 3.1.1.4) are a superfamily of enzymes that catalyse the hydrolysis of the *sn*-2 ester bond of phospholipids to release free fatty acids and lysophospholipids [1]. According to their localization, they are usually divided into intracellular and secreted enzymes. Secreted PLA_2s ($sPLA_2$s) are structurally related, Ca^{2+}-dependent and disulfide-rich 13–18-kDa proteins. The recent discovery of new groups of mammalian $sPLA_2$s and their receptors [2] has further increased interest in the physiological roles played by these PLA_2s. $sPLA_2$s are also found in venoms of different animals, such as insects, scorpions and snakes. Due to their structural similarity to the mammalian enzymes, the diverse snake venom $sPLA_2$s constitute a useful tool for investigating the interaction of PLA_2s with receptors.

Although they are structurally similar, snake venom $sPLA_2$s exhibit a great variety of pharmacological effects, including neurotoxicity, myotoxicity and anticoagulant activity. In spite of numerous attempts, their structure–activity relationships have not been resolved. Presynaptically acting $sPLA_2$ neurotoxins are the most potent toxins isolated from snake venoms, but the molecular basis of their toxicity is also not completely understood [3]. It is assumed that they first bind to different but specific receptors on the presynaptic membrane [4], after which they are presumably endocytosed [5,6]. In the nerve cell, they may interfere with the cycling of synaptic vesicles by binding to some target proteins [5] and by hydrolysing phospholipids [6]. The result of poisoning is an irreversible blockade of acetylcholine release at neuromuscular junctions leading to death of the prey due to paralysis of respiratory muscles [7].

Ammodytoxins A, B and C (Atxs) are monomeric $sPLA_2$s of group IIA with presynaptic neurotoxicity, isolated from the venom of the long-nosed viper, *Vipera ammodytes ammodytes*, with AtxA being the most toxic [8,9]. Two membrane-bound receptors for Atxs, R25 (25 kDa) and R180 (180 kDa), have been found in porcine cerebral cortex. R25 binds only Atxs [10], while R180, identified as an M-type $sPLA_2$ receptor, homologous to the macrophage mannose receptor, binds both toxic and nontoxic $sPLA_2$s of groups I and II [11,12]. In the course of purification of R25, a 16-kDa, high-affinity binding protein for AtxC was isolated and identified as calmodulin (CaM) [13].

CaM is a widely distributed protein, serving as a primary Ca^{2+} sensor in eukaryotic cells. It participates in different signalling pathways that regulate important biological

Correspondence to J. Pungerčar, Department of Biochemistry and Molecular Biology, Jožef Stefan Institute, Jamova 39, SI-1000 Ljubljana, Slovenia. Fax: +386 1257 3594, Tel.: +386 14773713, E-mail: joze.pungercar@ijs.si

Abbreviations: Atx, ammodytoxin; $AtxA^{KK}$, AtxA(Y115K/I116K) mutant; $AtxA^{KKML}$, AtxA(Y115K/I116K/R118M/N119L) mutant; CaM, calmodulin; $DPLA_2$, PLA_2 VIIIa from *Daboia russellii russellii*; $DPLA_2^{YIRN}$, $DPLA_2$(K115Y/K116I/M118R/L119N) mutant; PLA_2, phospholipase A_2; R25 and R180, receptors for Atxs in porcine cerebral cortex of 25 kDa and 180 kDa, respectively; $sPLA_2$, secreted PLA_2.

Enzyme: phospholipase A_2 (EC 3.1.1.4).

(Received 28 February 2003, revised 15 May 2003, accepted 20 May 2003)

processes such as growth, proliferation and movement [14], as well as vesicular fusion [15]. The identification of CaM as a potential target molecule in the presynaptic action of Atxs [13] raised the questions as to which part of the toxin is involved in this interaction and how the affinity for CaM is related to the neurotoxicity. As a search for typical CaM-binding sequence motifs [16,17] in Atxs that may be involved in CaM binding was not successful, we have approached this question by protein engineering.

We have shown previously that the C-terminal region of highly toxic AtxA is very important for presynaptic neurotoxicity [18–20]. The substitution of residues Y115, I116, R118 and N119 in AtxA with sequentially equivalent residues K, K, M and L, present in a weakly neurotoxic $sPLA_2$, VIIIa, from Russell's viper ($DPLA_2$) [21,22], dramatically decreased its lethal potency to the level of the latter [23]. In the present study, interaction of group IIA $sPLA_2$ toxins with CaM was evaluated using a set of AtxA mutants, including this quadruple (KKML) mutant, as well as recombinant $DPLA_2$ and its quadruple reciprocal (YIRN) mutant. Additionally, four peptides deduced from different regions of AtxA were analysed for their ability to compete with the toxin in binding to CaM. The results indicate that a novel CaM-binding site, which does not conform to known CaM-binding motifs, is located in the C-terminal part of AtxA, more specifically in the region 107–125.

Experimental procedures

Materials

AtxB and AtxC were isolated from *V. a. ammodytes* venom [24]. AtxA and its mutants (K108N/K111N and K128E, Y115K/I116K designated as $AtxA^{KK}$, Y115K/I116K/R118M/N119L designated as $AtxA^{KKML}$, K108N/K111N/K127T/K128E/E129T/K132E and K127T) were produced in *Escherichia coli* and purified as described [19,20,23]. Restriction enzymes were from MBI Fermentas (Vilnius, Lithuania) and New England BioLabs. Vent DNA polymerase, T4 polynucleotide kinase and *Taq* DNA ligase were from New England BioLabs. T4 DNA ligase was from Boehringer Mannheim. Hog brain CaM was from Roche Molecular Biochemicals and oligonucleotides from MWG-Biotech (Ebersberg, Germany). Radioisotopes were from Perkin-Elmer Life Sciences, and disuccinimidyl suberate from Pierce (Rockford, IL). All other chemicals were of analytical grade.

Construction of $DPLA_2$ and $DPLA_2^{YIRN}$ expression vectors

Two constructs coding for wild-type $DPLA_2$ from Russell's viper, *Daboia russellii russellii* [22], formerly known as *D. r. pulchella* [25], and its YIRN mutant were prepared by PCR-directed mutagenesis. The templates for PCR were the expression plasmids encoding either wild-type AtxA [19] for constructing the $DPLA_2^{YIRN}$ gene, or the $AtxA^{KKML}$ mutant [23] for constructing the $DPLA_2$ gene. The oligonucleotide primers used are shown in Table 1. Three PCR amplifications were performed in each case to obtain the first (fragment 1; using oligonucleotides 1+ and 1–), middle (fragment 2; using outer oligonucleotides 2+ and 2–, and inner oligonucleotides 2a+ and 2b+) and last part (fragment 3; oligonucleotides either $3+^{wt}$ or $3+^{YIRN}$, and 3–) of the genes. For synthesis of the fragments 1 and 3, the reaction mixture (100 μL) consisted of 50 pmol of each amplification primer, 400 μM of each of the four deoxyribonucleoside triphosphates, *Taq* DNA ligase buffer (New England BioLabs) and 100 ng of template DNA. Manual hot start amplification was performed with 1 U Vent polymerase after heating the mixture at 96 °C for 10 min The two PCRs consisted of 30 cycles of 95 °C for 1 min, 67 °C for 1 min and 72 °C for 1 min, with the final extension at 72 °C for 7 min. For synthesis of fragment 2, in addition to outer primers, two inner primers were included in the reaction. The inner primers (2a+ and 2b+) were first phosphorylated at their 5′ ends with T4 polynucleotide kinase according to manufacturer's instructions. They were added (50 pmol of each) to the PCR mixture, together with 1 U Vent polymerase and 80 U *Taq* ligase, as described [26]. The reactions consisted of 30 cycles of 94 °C for 30 s (first denaturation at 96 °C for 7 min), 49 °C for 1 min and 72 °C for 4 min. The PCR products were analysed on 1.7% (w/v) agarose gels, the desired fragments excised, purified with GeneClean II (BIO101,

Table 1. Oligonucleotide primers used for PCR-directed mutagenesis. Recognition sites for restriction endonucleases (*Hin*dIII, *Eco*RI, *Not*I, *Pst*I) used for construction are underlined. Nucleotides introducing mutations are shown in lower case letters; those resulting in amino acid substitutions (nonsynonymous) in bold, and silent mutations in normal type. Sense primers are designated by a plus (+) and antisense by minus (–) signs. The primer 1 + is complementary to the T7 promoter region, while other primers are complementary to the PLA_2-coding regions of the expression plasmids.

Primer	Sequence (5′ to 3′ end)
1+	TAATACGACTCACTATAGGGAGACCACAACGGTTTCC
1–	GGGC**aag**cTTCCCCGTCTCC**t**CCAGGATCATC**t**TCCCG
2+	GGGCAAG**cttg**CT**a**TT**c**CCTCCTACTCCT**c**TTACGGATGCTACTGCGGC**tg**GGGGGG
2a+	GACTGCA**a**CCCCAAA**t**CGGACAG
2b+	CAAATAC**aAg**CGGG**t**GAACGGGGCTATCGTCTGTG**a**AAAAGGC
2–	GGAATTCGCgGCcGCCtTGTCACACTCACAAATCCGATTCTC
$3+^{wt}$	GGGCAAGCTTGCgGCcGCAATCTGCTTTCGA**c**AGAATCTGAA**c**ACATA**ttcg**AAAAAGTATATGC
$3+^{YIRN}$	GGGCAAGCTTGCgGCcGCAATCTGCTTCCGA**c**AGAATCTGAA**c**ACATAC**Ag**CTATATATATAGG
3–	GGAATTCTGCAGTTAGCATTT**gag**CTC**tcc**CTTGCACAAgAAGTCCGG

Vista, CA), digested with *Bam*HI/*Hin*dIII (fragment 1, 60 bp), *Hin*dIII/*Eco*RI (fragment 2, 236 bp) and *Hin*dIII/*Eco*RI (fragment 3, 107 bp), respectively, and separately ligated into pUC19 vector. The sequences were confirmed by sequencing both strands of the PCR inserts using the ABI Prism 310 Genetic Analyser (Perkin-Elmer Applied Biosystems). The plasmids were digested with *Bam*HI/*Hin*dIII (fragment 1, 60 bp), *Hin*dIII/*Not*I (fragment 2, 229 bp) and *Not*I/*Pst*I (fragment 3, 95 bp), and the three fragments inserted in a single-step ligation between the *Bam*HI and *Pst*I restriction sites of the T7 RNA polymerase promoter-based vector [27], aimed for expression of AtxA, fused at its N terminus with a 13-amino acid residue peptide [19].

Bacterial expression and purification of recombinant toxins

E. coli BL21(DE3) (Novagen, Madison, WI) cells harbouring the expression plasmid (encoding either $DPLA_2$ or $DPLA_2^{YIRN}$) were allowed to grow at 37 °C to an OD_{600} of 2.0 in Luria–Bertani enriched medium (7×450 mL). Fusion protein expression was induced with 0.4 mM isopropyl thio-β-D-galactoside. Three hours later, bacteria were harvested by centrifugation. Isolation of inclusion bodies, protein refolding, activation and purification of the toxins were carried out as described for AtxA and its mutants [19,20].

Analytical methods

Protein samples were analysed by SDS/PAGE in the presence of 150 mM dithiothreitol using 15% (w/v) polyacrylamide gels and Coomassie brilliant blue R250 staining. Reverse-phase HPLC was performed using a HP1100 system (Hewlett-Packard, Waldbronn, Germany). The samples were loaded on an Aquapore 300 BU column (30×4.6 mm) equilibrated with 0.1% (v/v) trifluoroacetic acid and eluted with a linear gradient of 0–80% (v/v) acetonitrile at a flow rate of 1 $mL \cdot min^{-1}$. The N-terminal sequence was determined using an Applied Biosystems Procise 492 A protein sequencing system (Foster City, CA). Electrospray ionization MS was performed using a high-resolution magnetic-sector AutospecQ mass spectrometer (Micromass, Manchester, UK).

CD

CD spectra were recorded from 250 to 200 nm at 25 °C on an Aviv 62 A DS CD spectrometer. Bandwidth was 2 nm, step size 1 nm and averaging time 2 s. Protein concentrations were as follows: 13.9 μM for recombinant AtxA, 11.9 μM for wild-type $DPLA_2$ and 34.8 μM for $DPLA_2^{YIRN}$ mutant, all in water. Protein samples and water were scanned three times in a cell with 1 mm pathlength. The far-UV spectra were averaged and smoothed.

Enzymatic activity

PLA_2 activity on a micellar substrate was determined using a 718 STAT Titrino pH-stat (Metrohm, Herisau, Switzerland). The hydrolysis of egg-yolk PtdCho was measured in a reaction mixture (8 mL) supplemented with 1% (v/v) Triton X-100 and 15 mM $CaCl_2$, at pH 8.0 and 40 °C. The fatty acids released were titrated with 10 mM NaOH. One enzyme unit (U) corresponds to 1 μmol of hydrolysed phospholipid per minute.

Toxicity

Lethality was determined by intraperitoneal injection of 0.5 mL of each recombinant toxin in 0.9% (w/v) NaCl (concentrations ranging from 4 to 2400 $\mu g \cdot mL^{-1}$) into NMRI albino mice. Six dose levels and five mice per dose were used for each toxin. Neurotoxic effects on experimental animals were observed within 24 h, and LD_{50} was determined using a standard method [28]. All experimental procedures on mice were performed in accordance with the EC Council Directive regarding animal experimentation.

Binding studies

In protein binding studies, AtxC instead of more toxic AtxA was used due to the lower extent of nonspecific binding. AtxC was radioiodinated (^{125}I-AtxC) as previously reported [29]. CaM was dissolved in a 2.5 : 1 mixture of 140 mM 4-morpholineethanesulphonic acid pH 5.0, 200 mM NaCl, 4 mM $CaCl_2$, 0.2% (w/v) Triton X-100 (AtxC-CH Sepharose 4B elution buffer for R16) and 0.5 M triethanolamine pH 8.2, containing 150 mM NaCl [13]. The CaM (19 nM) solution, a fixed concentration of ^{125}I-AtxC (10 nM) and increasing concentrations of unlabeled competitor (recombinant or native toxin) were incubated at room temperature for 30 min with occasional vortexing. Toxins were cross-linked to their binding proteins by adding disuccinimidyl suberate, dissolved in dimethyl sulfoxide just before use, to a final concentration of 100 μM. The reaction mixture was mixed vigorously for 5 min at room temperature. The reaction was stopped by adding SDS/PAGE sample buffer containing dithiothreitol. Following electrophoresis and autoradiography, the intensities of the specific adducts on autoradiographs were quantified by QuantiScan (Biosoft, Cambridge, UK) and the data analysed using the nonlinear curve fitting program GraFit, Version 3.0 (Erithacus Software, Staines, UK).

Inhibition of cross-linking with synthetic peptides

Four peptides analysed were synthesized previously [30]. Their sequences correspond to four sequence segments of AtxA (L1 deduced from the amino acid region 113–121, L2 from 106 to 113, L3 from 70 to 78 and L4 from 125 to 133). 21 nM CaM in 75 mM Hepes, pH 8.2, 150 mM NaCl, 2.5 mM $CaCl_2$, 0.14% (w/v) Triton X-100 was incubated at room temperature with 0.8 mM concentration of either L1, L2, L3 or L4 peptide. For determination of the IC_{50} of the L1 peptide increasing concentrations of L1 were added in the range from 0 to 64 μM. After 30 min of incubation ^{125}I-AtxC was added, to a final concentration of 10 nM, and cross-linking performed as described above.

Results

Design, production and properties of recombinant $DPLA_2$s

To produce recombinant wild-type $DPLA_2$, 37 nucleotide nonsynonymous mutations in total were introduced into an AtxA-coding DNA template, resulting in substitution of 23 amino acid residues and deletion of one residue at the C terminus (Fig. 1). Its quadruple mutant ($DPLA_2^{YIRN}$), which is more similar to AtxA, was produced by 27 nucleotide nonsynonymous mutations. A few other, silent (synonymous) mutations were designed to introduce restriction sites (*Hin*dIII, *Not*I) that would support ligation of the three PCR fragments into each of the two $DPLA_2$ genes. Recombinant $DPLA_2$ toxins were produced in *E. coli* as nontoxic N-terminal fusion proteins in the form of insoluble inclusion bodies. Using a procedure developed for AtxA [19], they were successfully renatured, activated by limited trypsin digestion to remove the short N-terminal peptide (Fig. 2, lane 2), and purified to homogeneity in the active, correctly folded form. The final yield was about 6 mg of each recombinant toxin per litre of bacterial culture.

A single N-terminal protein sequence (^{1}SLLEF…) in both $DPLA_2$ toxins proved that the N-terminal fusion peptide was correctly removed and that no other cleavage occurred due to trypsin activation. Electrospray ionization MS confirmed the calculated molecular masses, 13 597 Da for $DPLA_2$ and 13 643 Da for $DPLA_2^{YIRN}$. The far-UV CD spectra of the two recombinant $DPLA_2$s were closely similar (Fig. 3), and similar to that of AtxA which differs from $DPLA_2$ in about 20% of amino acid residues, located mainly on the molecular surface. This indicates that the four substitutions (K115Y/K116I/M118R/L119N) introduced in $DPLA_2$ did not induce any significant conformational changes in the polypeptide backbone. The structural integrity of the fold is further supported by the specific

```
                .       .       .       .       .       .
AtxA    SLLEFGMMILGETG-KNPLTSYSFYGCYCGVGGKGTPKDATDRCCFVHDC    50
AtxB    ..............-....................................
AtxC    ..............-....................................
DPLA2   ......K...E...-.LAIP...S......W....................

                .       .         . L3    .       .       .
AtxA    CYGNLP--D-C-----SPKTDRYKYHRENGAIVCGK-GTSCENRICECDR   100
AtxB    ......--.-.-----.....................-.............
AtxC    ......--.-.-----.....................-.............
DPLA2   ......--.-.-----N..S.....K.V......E.-............K

                  N  N    KK ML    I  TET  E
                L2↑ ·↑ L1↑↑ ↑↑·   ↑L4↑↑↑· ↑
AtxA    AAAICFRKNLKTYNYIYRNYPD-FLCKKESEKC                  133
AtxB    ..............H..MY...-..........
AtxC    ......................-I...E.....
DPLA2   .......Q..N..SKK.ML...-....G.-L..
                      ↓↓ ↓↓
                      YI RN
```

Fig. 1. Amino acid alignment of Atxs with $DPLA_2$. The consensus numbering system of $sPLA_2$s is used (residues 1–133; according to [31]). Identical residues are represented by dots, and gaps introduced to optimize the alignment are shown by dashes. Arrows indicate amino acid substitutions in the C-terminal region of different mutants. The positions of four synthetic peptides (L1 to L4) are shown by underlining the corresponding regions in AtxA.

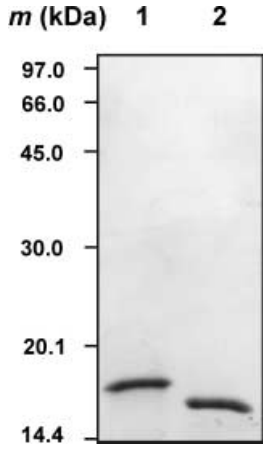

Fig. 2. SDS/PAGE analysis of recombinant $DPLA_2$. Wild-type $DPLA_2$ was purified as described in Experimental procedures. Fusion $DPLA_2$ (lane 1) and activated $DPLA_2$ (lane 2) were analysed on a 15% (w/v) polyacrylamide gels containing SDS and stained with Coomassie blue.

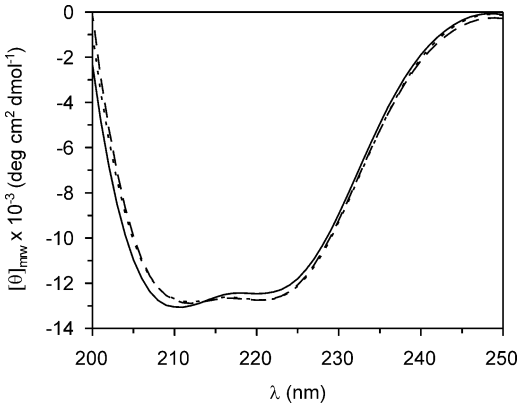

Fig. 3. CD spectra of recombinant $DPLA_2$s and AtxA. The far-UV CD spectra are shown for AtxA (solid line), wild-type $DPLA_2$ (long-dashed line) and $DPLA_2^{YIRN}$ mutant (short-dashed line). Measuring conditions are given in Experimental procedures.

enzymatic activities of both recombinant toxins, 760 $U \cdot mg^{-1}$ of $DPLA_2$ and 20 $U \cdot mg^{-1}$ of $DPLA_2^{YIRN}$.

Protein–protein interaction studies

To investigate the topology of binding of Atxs to the high-affinity binding protein, CaM, a number of AtxA mutants were tested (Table 2). These mutants, as well as wild-type AtxB and AtxC, differ from AtxA in the C-terminal residues which are located on the molecular surface (Fig. 4). All the AtxA mutants bound to CaM less strongly than AtxA (IC_{50} = 6 nM), with the lowest, eightfold lower, binding affinity being observed in the case of the quadruple mutant, $AtxA^{KKML}$. The measured IC_{50}s indicate that no single residue is critical for binding to CaM and that a relatively large surface of the toxin in the C-terminal part is involved in this interaction. The cluster of residues YIRN in the region 115–119 of AtxA appears to be particularly

Table 2. Binding affinity and toxicity of AtxA, $DPLA_2$ and their mutants. The IC_{50} values are means ± S.E. of at least three independent measurements.

$sPLA_2$	IC_{50} for CaM (nM)	LD_{50} ($\mu g \cdot kg^{-1}$)
AtxA		
Wild-type	6 ± 2	21[a]
K128E	14 ± 3	45[b]
K108N/K111N	17 ± 4	67[b]
K127T	20 ± 3	35[c]
F124I/K128E (AtxC)	21 ± 3	360[a]
Y115K/I116K ($AtxA^{KK}$)	21 ± 3	≈ 5000[d]
Y115H/R118M/N119Y (AtxB)	23 ± 4	580[a]
K108N/K111N/K127T/K128E/E129T/K132E	27 ± 5	660[c]
Y115K/I116K/R118M/N119L ($AtxA^{KKML}$)	50 ± 9	≈ 6000[d]
$DPLA_2$		
K115Y/K116I/M118R/L119N ($DPLA_2^{YIRN}$)	43 ± 14	≈ 17 000
Wild-type	300 ± 36	3100[e]

[a] [8], [b] [19], [c] [20], [d] [23], [e] LD_{50}, 5300 $\mu g \cdot kg^{-1}$ for native toxin, isolated from *Daboia russellii russellii* venom [21].

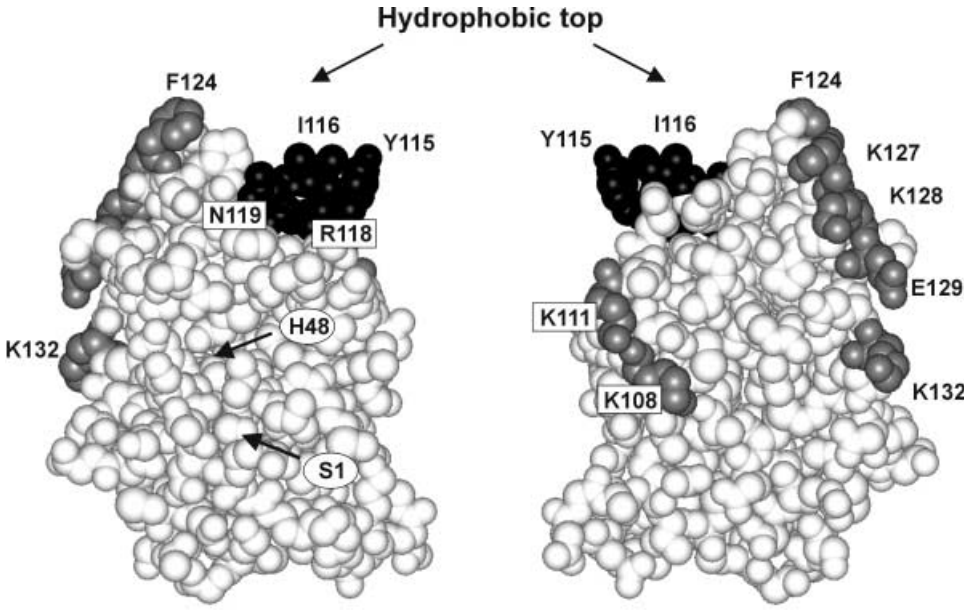

Fig. 4. Location of the mutations in AtxA. Two orientations of the molecule are shown. Left, the front view, with the N terminus (with Ser1) and active site pocket (with His48) facing the viewer and the β-structure on the right lower corner. Right, the back view, where the molecule is rotated by 180 degrees around its vertical axis. The YIRN cluster is shown in black, other residues substituted in AtxA mutants used in this study are shaded dark grey. The figure of the three-dimensional model of AtxA [19] was generated using WEBLAB VIEWERLITE software (Molecular Simulations, Cambridge, UK).

important for binding to CaM, which was confirmed by introducing the reverse substitutions in $DPLA_2$. The CaM-binding affinity of wild-type $DPLA_2$ was 50 times lower than that of AtxA. When the AtxA-specific residues (Y115, I116, R118 and N119) were introduced into the $DPLA_2$ molecule, its CaM-binding affinity was sevenfold higher and similar to that of the $AtxA^{KKML}$ mutant (Table 2, Fig. 5).

Relationship between protein binding affinity and toxicity

We were interested in the neurotoxic potency of recombinant $DPLA_2$s (Table 2) and to see if there is any correlation between the binding affinities of neurotoxic $sPLA_2$s to CaM and their lethal effect on mice. Lethality of the recombinant wild-type $DPLA_2$ (3.1 $mg \cdot kg^{-1}$) was slightly higher than that reported for the native toxin (5.3 $mg \cdot kg^{-1}$) isolated from the venom of Russell's viper [21], which may be the result of the different method of LD_{50} determination. Surprisingly, introduction of the YIRN cluster into $DPLA_2$ lowered its toxicity by a factor of 5.5 (LD_{50} increased from 3.1 to 17 $mg \cdot kg^{-1}$). Thus, no direct correlation is observed between the lethal potency of the 11 $sPLA_2$ toxins analysed in this study and their binding affinity for CaM. Nevertheless, all the highly toxic $sPLA_2$s also have a high affinity for CaM.

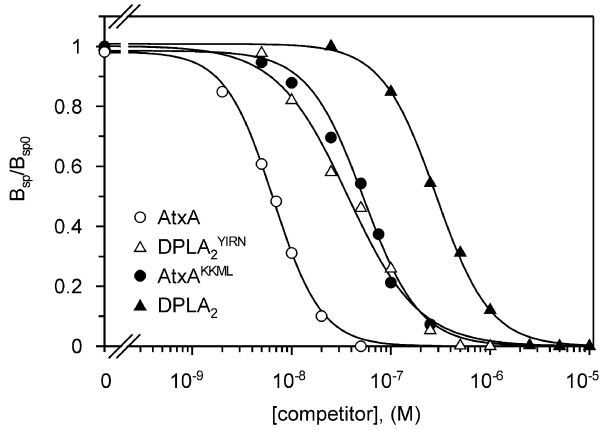

Fig. 5. Competition of recombinant PLA_2 toxins with ^{125}I-AtxC for binding to CaM. CaM was incubated with the labelled AtxC in the presence of increasing concentrations of the indicated competitor PLA_2 toxins, after which cross-linking and analysis of the products were performed as described in Experimental procedures. Radioactivity of the ^{125}I-AtxC-binding protein adduct was quantified and is shown relative to that in the absence of competitor. The values shown are means ± S.E. of at least three independent measurements.

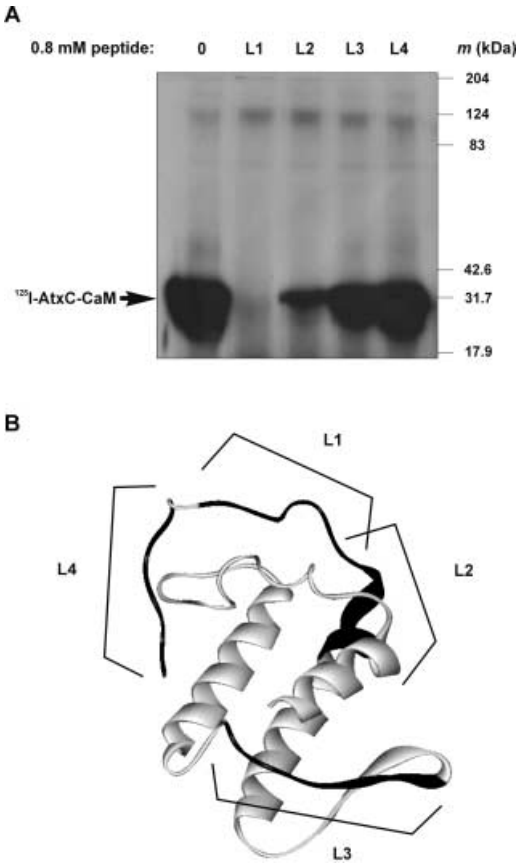

Fig. 6. Inhibition of cross-linking with synthetic peptides. (A) CaM and ^{125}I-AtxC were cross-linked in the absence (lane 0) or presence of the indicated peptides (lanes L1–L4). The products of cross-linking were analysed by electrophoresis on a 12.5% (w/v) polyacrylamide gel in the presence of SDS and 2-mercaptoethanol, followed by autoradiography. (B) Position of the synthetic peptides (L1, L2, L3 and L4; shown in black) in the structural model of AtxA. The protein backbone is shown in solid ribon representation. Orientation of the molecule is the same as that on the left side of Fig. 4.

Synthetic peptides have the ability to compete with AtxC for binding to CaM

The L1 peptide, derived from residues 113–121 of AtxA, completely inhibited the binding of ^{125}I-AtxC to CaM at 0.8 mM concentration (Fig. 6A). At the same concentration, partial inhibition was observed with the L2 peptide (residues 106–113), while the other two peptides, L3 (residues 70–78) and L4 (residues 125–133), had virtually no effect on this interaction. The IC_{50} of the L1 nonapeptide determined in the cross-linking competition experiment is 40 μM, which is about 2000 times higher than that of wild-type AtxC.

Discussion

In our previous study, we demonstrated a critical role for the C-terminal residues Y115, I116, R118 and N119 (the YIRN cluster) in the neurotoxicity of AtxA [23]. The set of eight AtxA mutants used in this study, including wild-type AtxB and AtxC, have shown that the same cluster is also significantly involved in binding to CaM. Several other hydrophobic (such as F124) and basic (such as K108, K111, K127, K128) residues from the C-terminal region, and also from the N-terminal region of AtxA, which are in the vicinity, as revealed by single-site mutations of F24 [32], appear to contribute to this interaction. All of these residues, which may interact with CaM, are spread over a large surface area on the molecule. This assumption is consistent with the high affinity of AtxA for CaM observed in inhibition of cross-linking (IC_{50} = 6 nM, which corresponds to a K_d of ≈ 3 nM).

Two natural isotoxins, AtxB and AtxC, bind to CaM three to four times less strongly than AtxA. AtxB differs from the most toxic AtxA by three residues, Y115H/R118M/N119Y, located within the YIRN cluster. These substitutions reduce the CaM-binding affinity of AtxB to the level of the $AtxA^{KK}$ mutant, but less than that of the $AtxA^{KKML}$ mutant. We were also interested in analysing the relative contribution of hydrophobic or basic residues at positions 118 and 119 in the YIRN cluster to CaM binding, but our attempts to produce double mutants of AtxA with hydrophobic residues at positions 118 (Met) and 119 (Leu or Phe) failed due to unsuccessful refolding *in vitro* of the recombinant proteins (G. Ivanovski, unpublished results).

The significant role of the YIRN cluster for binding to CaM was confirmed by introducing the reverse substitution (KKML to YIRN) into $DPLA_2$, which substantially increased binding of $DPLA_2$ to CaM. The importance of the C-terminal part of AtxA including this cluster for interaction with CaM has also been demonstrated by our recent study on two chimeric proteins of a nontoxic $sPLA_2$, ammodytin I_2, with AtxA [33].

The proposed location of the CaM-binding site in AtxA is further supported by additional mapping with four synthetic peptides (see Fig. 6). Although the mapping may not be complete, it pointed to the very same region of the

toxin molecule where the YIRN cluster is located. It has been shown that Atxs interact only with the Ca^{2+}-bound form of CaM, with a stoichiometry of 1 : 1 [13]. The careful sequence analysis of AtxA that we performed has not identified any of the characteristic Ca^{2+}-dependent CaM-binding motifs [16,17,34]. There is only an apparent similarity to the 1–14 motif (based on the spacing of the bulky hydrophobic residues, such as F, I, L, V and W, within the motif), in which hydrophobic positions 1 and 14 would be occupied in AtxA and AtxB by L110 and F124, and in AtxC by L110 and I124 (see Fig. 1). Conventional CaM-binding motifs have been found in the regions of target proteins with the ability to form amphipathic α-helices [17], which cannot be the case of the C-terminal region of Atxs. This region lacks any appreciable α-helical structure, as seen in the highly conserved three-dimensional structures of group IIA $sPLA_2$s, including the recently determined structure of $DPLA_2$ [35]. In the three-dimensional model of AtxA (Fig. 4), the C-terminal region, bending over the top of the molecule, exposes a distinct hydrophobic patch formed by L110, I116 (within the YIRN cluster), P121, F124 and L125. This hydrophobic surface, surrounded by certain basic residues in the vicinity (such as K108, K111, K127 and K128), may constitute a novel CaM-binding site. Based on the peptide mapping of the surface-exposed residues, including the hydrophobic patch at the top of the molecule, the CaM-binding site in the C-terminal part of Atxs appears to reside within the region 107–125.

In the dumbbell conformation of CaM, where all four Ca^{2+}-binding sites are occupied, both the N- and C-terminal domain hydrophobic pockets are exposed for interaction with a variety of target molecules [36,37]. The structure of a complex between the Ca^{2+}-bound form of CaM and a CaM-binding peptide showed that hydrophobic interactions predominate over electrostatic ones in the binding [38], which may also be the case in the interaction of CaM with Atxs. It seems reasonable to assume that AtxA could bind with its C-terminal hydrophobic surface to one of these two hydrophobic, methionine-rich pockets in CaM. As this hydrophobic surface in the toxin molecule is surrounded by several basic residues, their presumed interaction with a rim of mostly negative charged residues surrounding each of the methionine-rich pockets of CaM [39] may help in orienting both molecules and contribute to the binding affinity. The AtxC–CaM complex recognized by CaM-specific monoclonal antibodies directed to the last 20 residues [13] indicates that this portion of the C-terminal domain of CaM is exposed in the complex, which favors involvement of the N-terminal methionine-rich pocket of CaM in the interaction with the toxin. The recent structures of CaM complexed with domains of the target proteins, such as the gating domain of a Ca^{2+}-activated K^+ channel [40] and the C-terminal part of toxic *Bacillus anthracis* oedema factor [41], suggest that interaction of CaM with larger proteins may be quite different from that observed with short helical peptides (of about 20 residues). Although the molecular mass of AtxA (13.8 kDa) is comparable to that of CaM (16.6 kDa), this does not exclude the possibility of tighter binding of highly flexible CaM on a larger area of the toxin surface, including some regions not identified by the present study.

Although all the highly neurotoxic $sPLA_2$s bound with high affinity to CaM, no direct correlation was observed in our experiments between the toxic potency of the $sPLA_2$ toxins and their binding affinity for CaM. For example, the substantial increase in the binding affinity for CaM observed by introducing the YIRN cluster into $DPLA_2$ was not accompanied by higher toxicity. On the contrary, its lethality was even lower, which indicates that some other site on the molecule should additionally contribute to neurotoxicity. It has been observed that, in addition to Atxs, $DPLA_2$ and their mutants, also other neurotoxic $sPLA_2$s of group IIA such as agkistrodotoxin and crotoxin are able to bind CaM [13], which supports its potential role in the process of neurotoxicity.

In conclusion, our results contribute to understanding the binding of AtxA, a member of group IIA $sPLA_2$ neurotoxins, to CaM. A nonconventional CaM-binding site identified in the C-terminal region of the toxin, which does not conform to previously known CaM-binding motifs, also adds to the emerging awareness of the wide repertoire of CaM–protein interactions in which this ubiquitous and highly conserved eukaryotic protein may be involved.

Acknowledgements

We would like to thank Dr B. Kralj for molecular mass analysis, Dr T. Malovrh for help in lethality measurements and Dr R.H. Pain for critical reading of the manuscript. This work was supported by grant P0-0501-0106 from the Slovenian Ministry of Education, Science and Sport.

References

1. Six, D.A. & Dennis, E.A. (2000) The expanding superfamily of phospholipase A_2 enzymes: classification and characterization. *Biochim. Biophys. Acta – Mol. Cell. Biol. Lipids* **1488**, 1–19.
2. Valentin, E. & Lambeau, G. (2000) Increasing molecular diversity of secreted phospholipases A_2 and their receptors and binding proteins. *Biochim. Biophys. Acta – Mol. Cell. Biol. Lipids* **1488**, 59–70.
3. Gubenšek, F., Križaj, I. & Pungerčar, J. (1997) Monomeric phospholipase A_2 neurotoxins. In: *Venom Phospholipase A_2 Enzymes: Structure, Function and Mechanism* (Kini, R.M., ed.), pp. 245–268. John Wiley & Sons, Chichester, UK.
4. Chang, C.C. & Su, M.J. (1980) Mutual potentiation, at nerve terminals, between toxins from snake venoms which contain phospholipase A activity: β-bungarotoxin, crotoxin, taipoxin. *Toxicon* **18**, 641–648.
5. Križaj, I. & Gubenšek, F. (2000) Neuronal receptors for phospholipases A_2 and β-neurotoxicity. *Biochimie* **82**, 807–814.
6. Montecucco, C. & Rossetto, O. (2000) How do presynaptic PLA_2 neurotoxins block nerve terminals? *Trends Biochem. Sci.* **25**, 266–270.
7. Chang, C.C. (1985) Neurotoxins with phospholipase A_2 activity in snake venoms. *Proc. Natl Sci. Counc. B ROC* **9**, 126–142.
8. Thouin, L.G., Jr, Ritonja, A., Gubenšek, F. & Russell, F.E. (1982) Neuromuscular and lethal effects of phospholipase A from *Vipera ammodytes* venom. *Toxicon* **20**, 1051–1058.
9. Lee, C.Y., Tsai, M.C., Chen, Y.M., Ritonja, A. & Gubenšek, F. (1984) Mode of neuromuscular blocking action of toxic phospholipases A_2 from *Vipera ammodytes* venom. *Arch. Int. Pharmacodyn. Ther.* **268**, 313–324.
10. Vučemilo, N., Čopič, A., Gubenšek, F. & Križaj, I. (1998) Identification of a new high-affinity binding protein for neurotoxic

phospholipases A_2. *Biochem. Biophys. Res. Commun.* **251**, 209–212.
11. Čopič, A., Vučemilo, N., Gubenšek, F. & Križaj, I. (1999) Identification and purification of a novel receptor for secretory phospholipase A_2 in porcine cerebral cortex. *J. Biol. Chem.* **274**, 26315–26320.
12. Vardjan, N., Sherman, N.E., Pungerčar, J., Fox, J.W., Gubenšek, F. & Križaj, I. (2001) High-molecular-mass receptors for ammodytoxin in pig are tissue-specific isoforms of M-type phospholipase A_2 receptor. *Biochem. Biophys. Res. Commun.* **289**, 143–149.
13. Šribar, J., Čopič, A., Pariš, A., Sherman, N.E., Gubenšek, F., Fox, J.W. & Križaj, I. (2001) A high affinity acceptor for phospholipase A_2 with neurotoxic activity is a calmodulin. *J. Biol. Chem.* **276**, 12493–12496.
14. Chin, D. & Means, A.R. (2000) Calmodulin: a prototypical calcium sensor. *Trends Cell Biol.* **10**, 322–328.
15. Peters, C. & Mayer, A. (1998) Ca^{2+}/calmodulin signals the completion of docking and triggers a late step of vacuole fusion. *Nature* **396**, 575–580.
16. O'Neil, K.T. & DeGrado, W.F. (1990) How calmodulin binds its targets: sequence independent recognition of amphiphilic α-helices. *Trends Biochem. Sci.* **15**, 59–64.
17. Rhoads, A.R. & Friedberg, F. (1997) Sequence motifs for calmodulin recognition. *FASEB J.* **11**, 331–340.
18. Križaj, I., Ritonja, A., Turk, D. & Gubenšek, F. (1989) Primary structure of ammodytoxin C further reveals the toxic site of ammodytoxin. *Biochim. Biophys. Acta* **999**, 198–202.
19. Pungerčar, J., Križaj, I., Liang, N.-S. & Gubenšek, F. (1999) An aromatic, but not a basic, residue is involved in the toxicity of group-II phospholipase A_2 neurotoxins. *Biochem. J.* **341**, 139–145.
20. Prijatelj, P., Čopič, A., Križaj, I., Gubenšek, F. & Pungerčar, J. (2000) Charge reversal of ammodytoxin A, a phospholipase A_2-toxin, does not abolish its neurotoxicity. *Biochem. J.* **352**, 251–255.
21. Kasturi, S. & Gowda, V.T. (1989) Purification and characterization of a major phospholipase A_2 from Russell's viper (*Vipera russelli*) venom. *Toxicon* **27**, 229–237.
22. Gowda, V.T., Schmidt, J. & Middlebrook, J.L. (1994) Primary sequence determination of the most basic myonecrotic phospholipase A2 from the venom of *Vipera russelli*. *Toxicon* **32**, 665–673.
23. Ivanovski, G., Čopič, A., Križaj, I., Gubenšek, F. & Pungerčar, J. (2000) The amino acid region 115–119 of ammodytoxins plays an important role in neurotoxicity. *Biochem. Biophys. Res. Commun.* **276**, 1229–1234.
24. Gubenšek, F., Ritonja, A., Zupan, J. & Turk, V. (1980) Baic proteins of *Vipera ammodytes* venom. Studies of structure and function. *Period. Biol.* **82**, 443–447.
25. Wüster, W., Golay, P. & Warrell, D.A. (1997) Synopsis of recent developments in venomous snake systematics. *Toxicon* **35**, 319–340.
26. Michael, S.F. (1994) Mutagenesis by incorporation of a phosphorylated oligo during PCR amplification. *Biotechniques* **16**, 410–412.
27. Tabor, S. (1990) Expression using the T7 RNA polymerase promotor system. In: *Current Protocols in Molecular Biology* (Ausubel, F.A., Brent, R., Kingston, R.E., Moore, D.D., Seidman, J.G., Smith, J.A. & Struhl, K., eds), pp. 16.2.1–16.2.5. Greene Publishing and Wiley-Interscience, New York.
28. Reed, L.J. & Muench, H. (1938) A simple method of estimating fifty per cent endpoints. *Am. J. Hygiene* **27**, 493–497.
29. Križaj, I., Dolly, J.O. & Gubenšek, F. (1994) Identification of the neuronal acceptor in bovine cortex for ammodytoxin C, a presynaptically neurotoxic phospholipase A_2. *Biochemistry* **33**, 13938–13945.
30. Čurin-Šerbec, V., Novak, D., Babnik, J., Turk, D. & Gubenšek, F. (1991) Immunological studies of the toxic site in ammodytoxin A. *FEBS Lett.* **280**, 175–178.
31. Renetseder, R., Brunie, S., Dijkstra, B.W., Drenth, J. & Sigler, P.B. (1985) A comparison of the crystal structures of phospholipase A_2 from bovine pancreas and *Crotalus atrox* venom. *J. Biol. Chem.* **260**, 11627–11634.
32. Petan, T., Križaj, I., Gubenšek, F. & Pungerčar, J. (2002) Phenylalanine-24 in the N-terminal region of ammodytoxins is important for both enzymic activity and presynaptic toxicity. *Biochem. J.* **363**, 353–358.
33. Prijatelj, P., Križaj, I., Kralj, B., Gubenšek, F. & Pungerčar, J. (2002) The C-terminal region of ammodytoxins is important but not sufficient for neurotoxicity. *Eur. J. Biochem.* **269**, 5759–5764.
34. Hoeflich, K.P. & Ikura, M. (2002) Calmodulin in action: diversity in target recognition and activation mechanisms. *Cell* **108**, 739–742.
35. Chandra, V., Kaur, P., Srinivasan, A. & Singh, T.P. (2000) Three-dimensional structure of a presynaptic neurotoxic phospholipase A_2 from *Daboia russelli pulchella* at 2.4 Å resolution. *J. Mol. Biol.* **296**, 1117–1126.
36. Ikura, M., Clore, G.M., Gronenborn, A.M., Zhu, G., Klee, C.B. & Bax, A. (1992) Solution structure of a calmodulin-target peptide complex by multidimensional NMR. *Science* **256**, 632–638.
37. Osawa, M., Swindells, M.B., Tanikawa, J., Tanaka, T., Mase, T., Furuya, T. & Ikura, M. (1998) Solution structure of calmodulin-W-7 complex: the basis of diversity in molecular recognition. *J. Mol. Biol.* **276**, 165–176.
38. Meador, W.E., Means, A.R. & Quiocho, F.A. (1992) Target enzyme recognition by calmodulin: 2.4 Å structure of a calmodulin-peptide complex. *Science* **257**, 1251–1255.
39. Chattopadhyaya, R., Meador, W.E., Means, A.R. & Quiocho, F.A. (1992) Calmodulin structure refined at 1.7 Å resolution. *J. Mol. Biol.* **228**, 1177–1192.
40. Schumacher, M.A., Rivard, A.F., Bachinger, H.P. & Adelman, J.P. (2001) Structure of the gating domain of a Ca^{2+}-activated K^+ channel complexed with Ca^{2+}/calmodulin. *Nature* **410**, 1120–1124.
41. Drum, C.L., Yan, S.Z., Bard, J., Shen, Y.Q., Lu, D., Soelaiman, S., Grabarek, Z., Bohm, A. & Tang, W.J. (2002) Structural basis for the activation of anthrax adenylyl cyclase exotoxin by calmodulin. *Nature* **415**, 396–402.